ELSEVIER

Surface Science 305 (1994) 307–311

surface science

Valence band Landau level mixing and anisotropy in $Si_{1-x}Ge_x$ investigated by resonant magnetotunneling

A. Zaslavsky *, D.A. Grützmacher, S.Y. Lin, T.P. Smith III, T.O. Sedgwick

IBM Research Division, T.J. Watson Research Center, Yorktown Heights, NY 10598, USA

(Received 16 April 1993; accepted for publication 4 June 1993)

Abstract

We report magnetotunneling measurements on strained p-Si/$Si_{1-x}Ge_x$ double-barrier resonant tunneling structures in fields up to 30 T. In the $I(V, B_\parallel)$ characteristics of the first heavy-hole peak we observe satellite resonances corresponding to tunneling with $\Delta n = 1$ and $\Delta n = 2$ changes in Landau index n. The relative intensity of the satellite peaks excludes scattering as a possible mechanism and we attribute the $\Delta n = 1$, 2 peaks to elastic tunneling made possible by Landau level mixing. The observed strong $\Delta n = 2$ mixing could arise from the large $E(k_\perp)$ anisotropy in the $Si_{1-x}Ge_x$ quantum well, which we probe by $I(V, B_\perp)$ measurements. From the shifts in the heavy-hole peak with in-plane $B_\perp$ orientation we find that at large $k_\perp$ the in-plane mass varies strongly between the $\langle 110 \rangle$ (heavy) and $\langle 100 \rangle$ (light) crystallographic directions.

Resonant magnetotunneling in double-barrier resonant tunneling structures (DBRTS) has become a powerful technique for probing two-dimensional (2D) subband states in quantum wells. If the tunneling carriers are described by a single, isotropic, parabolic band, like electrons in III–V heterostructures, the effects of a magnetic field parallel ($B_\parallel$) and transverse ($B_\perp$) to the tunneling direction are well understood. In a $B_\parallel$ field, the states are constrained into evenly spaced Landau levels with in-plane harmonic oscillator wavefunctions $\phi_n(r_\perp)$. The energy E and transverse momentum $k_\perp$ conservation rules that govern tunneling from the emitter into the well at $B = 0$ [1] are transformed into the conservation of E and Landau index n [2,3]. As Landau levels successively align, the peak acquires a weak staircase-like structure [3], but in the absence of scattering or LO-phonon emission [4] $B_\parallel$ cannot produce any structure in $I(V, B_\parallel)$ beyond the resonant peak. Conversely, in a $B_\perp$ field, the energies and densities of states of the 2D subbands in the well are not strongly affected if the magnetic length is larger than the well width W. The main $B_\perp$-induced effect is the peak broadening and shifting to higher bias due to the $\Delta k_\perp = eB_\perp \langle z \rangle / \hbar$ change in $k_\perp$ as the carrier tunnels a distance $\langle z \rangle$ from the emitter into the well [5,6]. If the in-plane dispersion $E(k_\perp)$ is isotropic, the peak shift ΔV is obviously independent of $B_\perp$ orientation in the plane; from E and $k_\perp$ conservation $\Delta V \sim B_\perp^2$ [5–7].

If the tunneling carriers cannot be described by a parabolic band, as in the case of p-type

* Corresponding author.

SSDI 0039-6028(93)E0702-V

III–V [8,9] and $Si/Si_{1-x}Ge_x$ [10,11] DBRTS, magnetic field effects are more complex. Hole states in quantum wells belong to interacting heavy-hole (HH) and light-hole (LH) bands with nonparabolic and anisotropic dispersion; there are additional strain-induced complications in $Si/Si_{1-x}Ge_x$ structures. We have measured $I(V, B_\parallel)$ to elucidate the valence band HH Landau level structure and $I(V, B_\perp)$ to probe the in-plane valence band anisotropy of strained $Si_{1-x}Ge_x$ quantum wells. In $I(V, B_\parallel)$ characteristics we find strong Landau index-nonconserving satellite peaks in the first heavy-hole (HH_0) resonance, which we interpret as the first observation of Landau level mixing [12–14] in transport. In the $I(V, B_\perp)$ data we find a strong dependence of peak bias on $B_\perp$ orientation with respect to crystallographic axes: in the HH_0 subband the in-plane mass $m_\perp^*$ is heavy along the $\langle 110 \rangle$ and light along the $\langle 100 \rangle$ axes.

Our p-$Si/Si_{1-x}Ge_x$ DBRTS were grown by atmospheric pressure CVD, with 50 Å Si barriers cladding the $Si_{0.75}Ge_{0.25}$ wells of thickness $W = 35$ and 23 Å, and the double-barrier structure in turn surrounded by graded $Si_{1-x}Ge_x$ emitter and collector regions (see Ref. [15] for details of the sample design and growth). The calculated DBRTS band diagram of the $W = 35$ Å device under bias is shown in Fig. 1a; the zero-field $I(V)$ characteristics of the two structures at $T = 4.2$ K are shown in Fig. 1b. Since the heavy–light hole strain splitting in $Si_{0.75}Ge_{0.25}$ $\Delta\epsilon \approx 40$ meV $\gg kT$, only the heavy-hole states are occupied in the emitter, and the $I(V)$ curves exhibit resonant peaks corresponding to the tunneling of emitter heavy holes into the HH_0 and LH_0 subbands in the well. The peak-to-valley ratios are high for p-type DBRTS, reaching 4 : 1 for LH_0 peaks. The expected threshold and peak voltages for the resonances are also shown in Fig. 1b: we employed interpolated SiGe valence band parameters to calculated the energies of the HH_0 and LH_0 subbands; assumed the same parabolic $E(k_\perp)$ for the emitter and the HH_0 subband; took the LH_0 subband to be dispersionless [16]; and applied the standard E and $k_\perp$ conservation rules [1]. Even in this naive model the agreement between the calculated and measured HH_0 peak positions is excellent. For the LH_0 peak the agreement is poor and a proper calculation of the LH_0 dispersion is clearly necessary.

The $I(V, B_\parallel)$ characteristics of the HH_0 peak in the $W = 35$ Å DBRTS for increasing up to 30 T are shown in Fig. 2. While the main HH_0 peak position remains nearly unchanged at $V_p = 140$ mV, already at $B_\parallel = 7.5$ T a weak shoulder appears at higher bias. As $B_\parallel$ increases, this shoulder develops into a strong satellite that shifts to higher V and dominates the main peak when $B_\parallel = 30$ T, while for $B_\parallel \geq 20$ T another, weaker

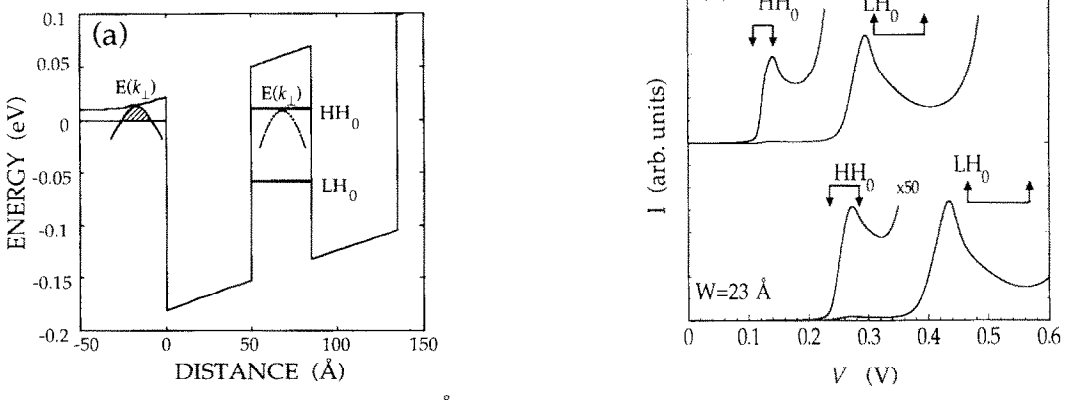

Fig. 1. (a) Calculated potential distribution of $W = 35$ Å DBRTS under bias $V = 140$ mV, with schematic $E(k_\perp)$ dispersion in the emitter and the HH_0 2D subband (occupied emitter states are hatched). (b) Tunneling $I(V, B = 0)$ characteristics at $T = 4.2$ K of structures with $W = 23$ and 35 Å. Arrows show the calculated threshold and peak voltages for the HH_0 and LH_0 peaks.

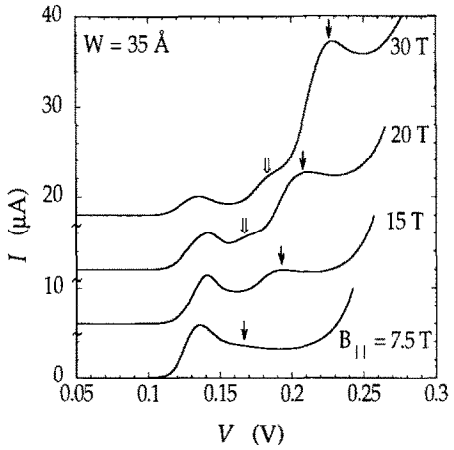

Fig. 2. $I(V, B_{\|})$ characteristics at $T = 4.2$ K of the $W = 35$ Å structure at $B_{\|} = 7.5$, 15, 20 and 30 T (curves displaced by 6 μA for clarity). Solid ($\Delta n = 2$) and open ($\Delta n = 1$) arrows mark the Landau index nonconserving peaks.

satellite feature appears in between. The $W = 23$ Å structure exhibits analogous behavior, with a stronger and a weaker satellite peaks shifting to higher bias with increasing $B_{\|}$.

The main and satellite peak positions of the HH_0 lineshape are summarized in Fig. 3. Since the satellite peaks occur at higher bias than the main HH_0 peak, they must arise from Landau index-nonconserving processes. From the $B_{\|}$-induced shifts in satellite peak positions, we attribute the stronger satellite to $\Delta n = 2$ tunneling and the weaker satellite to $\Delta n = 1$ tunneling. A possible mechanism for these index-nonconserving peaks is scattering, which was invoked by Schuberth et al. [17] to explain weak features observed in the conductance of the LH_0 peak in similar p-Si/$Si_{1-x}Ge_x$ DBRTS. Yet the strength of the $\Delta n = 2$ satellite, which exceeds the main peak at high $B_{\|}$, together with the relative weakness of the $\Delta n = 1$ satellite make a scattering mechanism unlikely. Although interface and impurity scattering can relax $k_{\perp}$ conservation or, equivalently, Landau index conservation [17], it is unlikely to produce satellite peaks comparable in strength to the main, index-conserving peak. Moreover, the $\Delta n = 1$ satellite is much weaker than $\Delta n = 2$, although the required change in $k_{\perp}$ for $\Delta n = 2$ tunneling is much larger if scattering is responsible. Consequently, instead of scattering-assisted tunneling, we interpret our data in terms of valence band Landau level mixing, which allows $\Delta n \neq 0$ tunneling.

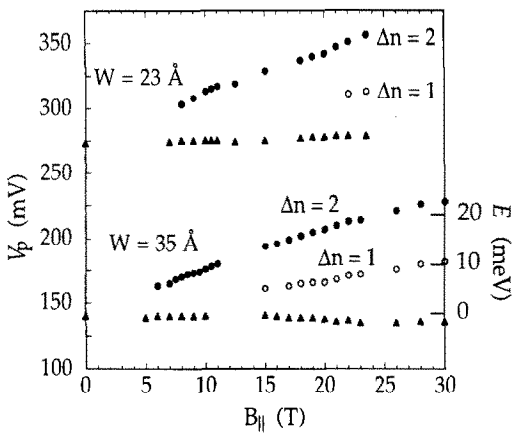

Fig. 3. Bias positions of the main (triangles) and satellite ($\Delta n = 1$, open circles; $\Delta n = 2$, filled circles) peaks versus $B_{\|}$. At right is the calculated energy scale of the Landau spectrum for the $W = 35$ Å device; the zero of energy is arbitrarily set to the HH_0 peak position at $B_{\|} = 0$.

Essentially, our DBRTS in a $B_{\|}$ field is described by an effective 4×4 Hamiltonian H_{ij} in the $|Jm_j\rangle$ basis [12–14]: $J = 3/2$; the quantization axis is $z \| B_{\|}$; $i, j = 1, 2, 3, 4$ label the states $m_j = 3/2, 1/2, -1/2, -3/2$ in that order; uniaxial strain contributes only to diagonal elements H_{ii} and splits the $|3/2 \pm 3/2\rangle$ (HH) and $|3/2 \pm 1/2\rangle$ (LH) bands by $\Delta\epsilon$ [13]. In a magnetic field, all H_{ij} elements can be expressed in terms of harmonic oscillator raising and lowering operators a and a_+. If the anisotropy term $(\gamma_3 - \gamma_2)a_+^2$ is ignored in the Hamiltonian, the four-component Landau level eigenfunctions Ψ_n can be written as a superposition of harmonic oscillator wavefunctions $\phi_n(r_{\perp})$ [12,14]:

$$\Psi_n^{l,h} = [\zeta_{1,n}\phi_{n-2};\ \zeta_{2,n}\phi_{n-1};\ \zeta_{3,n}\phi_n;\ \zeta_{4,n}\phi_{n+1}], \quad (1)$$

where $\zeta_{i,n}(z)$ are linear combinations of products $c_i(z)|Jm_j\rangle$, with $c_i(z)$ determined by the boundary conditions on Ψ_n. The diagonal H_{ii} terms have the form $(aa_+ + 1/2)$ and would give rise to separate sets of heavy and light-hole Landau lev-

els with linear $B_{\|}$ dependence, while the off-diagonal terms cause Landau level mixing. The relevant terms for $\Delta n = 2$ level mixing are $H_{13} \sim (\gamma_3 + \gamma_2)a^2 + (\gamma_3 - \gamma_2)a_+^2$; for $\Delta n = 1$ mixing they are $H_{12} \sim k_z a$ [14]. These terms mix oscillator functions $\phi_m(r_\perp)$ into the nth Landau level wavefunctions, where $m = n$, $n \pm 1$, $n \pm 2$ (the closed form wavefunction (1) is no longer valid when the anisotropy term is included, but $\phi_n(r_\perp)$ remain the basis from which the Landau level Ψ_n are constructed). In a bulk crystal the common ϕ_m of different Landau levels are multiplied by different orthogonal $|J\, m_j\rangle$ functions, making n a constant of motion, but in a DBRTS the boundary conditions at the barrier interfaces [14] make $\zeta_{i,n}(z)$ nonorthogonal at different z, allowing elastic tunneling from emitter to well between Landau levels with $\Delta n = 1,2$.

The $I(V, B_{\|})$ curves of Fig. 2 make it possible to obtain the separation between Landau levels by converting the voltage splitting between the main and satellite peaks into an energy scale, as done in Fig. 3 for the $W = 35$ Å device. At low and moderate $B_{\|}$ the $\Delta n = 2$ peak shifts linearly with $B_{\|}$. If we take this energy separation as a measure of heavy-hole in-plane mass we obtain $m_\perp^* = 0.29 \pm 0.04$, heavier than predicted by interpolated valence band parameters, but in agreement with recent cyclotron resonance measurements on $Si_{1-x}Ge_x$ quantum wells [18].

Without a true calculation of the mixed Landau level wavefunctions (1) in the quantum well our understanding of the relative strength of the $\Delta n \neq 0$ satellite peaks remains qualitative. From the data in Fig. 2, we find that mixing with $\Delta n = 1$ is about an order of magnitude weaker than $\Delta n = 2$. The weakness of $\Delta n = 1$ satellite is consistent with the relevant $H_{12} \sim k_z a$ term, since the resonant peaks occur when the 2D subbands are nearly aligned with the top of the band in the emitter (see Fig. 1a), so k_z is small [1]. The strong $\Delta n = 2$ mixing we observe could imply a strong in-plane anisotropy described by the $(\gamma_3 - \gamma_2)a_+^2$ term, especially since $\Delta n = 2$ tunneling was not observed in III–V DBRTS [9]. We tested this hypothesis by performing $I(V, B_\perp)$ measurements versus in-plane $B_\perp$ orientation, analogously to the earlier study by Gennser et al. [19] who reported $B_\perp$ orientation dependence of peak positions in MBE-grown $Si/Si_{1-x}Ge_x$ DBRTS.

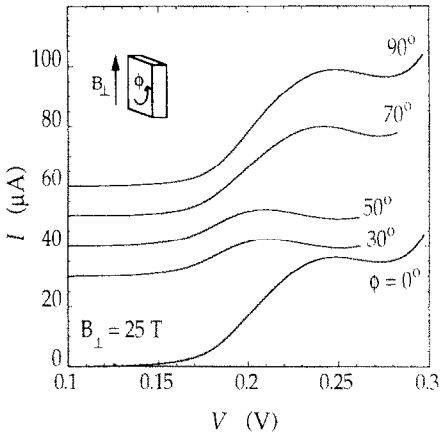

Fig. 4. $I(V, B_\perp = 25\ \text{T})$ HH_0 peak of the $W = 35$ Å DBRTS versus angle ϕ between $B_\perp$ and the $\langle 100 \rangle$ axis (curves displaced for clarity). Inset contains the measurement geometry.

Fig. 4 shows the strong variation in the HH_0 peak as a function of the angle ϕ between $B_\perp = 25$ T and the $\langle 100 \rangle$ axis in the $W = 35$ Å DBRTS, together with the measurement geometry (inset). The $B_\perp$-induced peak shift ΔV varies from $\Delta V \approx 110$ mV when $\phi = 0°$ ($B_\perp \| \langle 100 \rangle$ axis) to $\Delta V \approx 75$ mV when $\phi = 50°$ ($B_\perp \| \langle 110 \rangle$). The observed anisotropy, which is summarized for the $W = 35$ Å structure in Fig. 5, follows the crystal symmetry, with the largest ΔV occurring whenever $B_\perp$ is aligned with a $\langle 100 \rangle$ axis. By the simple geometrical construction in the inset of Fig. 5, showing schematically the states that can tunnel conserving E and $k_\perp$, assuming parabolic $E(k_\perp)$ dispersion with different curvature (different $m_\perp^*$) along $\langle 100 \rangle$ and $\langle 110 \rangle$, we immediately find that the effective heavy-hole mass $m_\perp^*$ away from the $k = 0$ band edge is markedly heavier along the $\langle 110 \rangle$ than the $\langle 100 \rangle$ axes. Due to band nonparabolicity further calculations are required to convert magnetotunneling data into real dispersion curves, but the $E(k_\perp)$ constant energy contour obtained by converting $\Delta V(\phi)$ into an energy scale is consistent with the $m_\perp^* \approx 0.29$ result obtained from $I(V, B_\perp)$ measurements that average over all $k_\perp$.

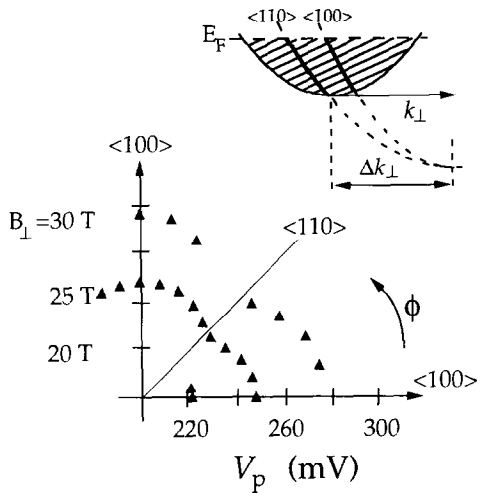

Fig. 5. HH_0 peak position V_p versus ϕ for $B_\perp = 20$, 25, 30 T in $W = 35$ Å DBRTS. Inset, schematic alignment of emitter and HH_0 states with parabolic $E(k_\perp)$ of different curvatures for two crystallographic directions. States that can tunnel elastically are shown in boldtype.

In conclusion, we have experimentally observed satellite peaks in the heavy-hole $I(V, B_\parallel)$ characteristics of $Si/Si_{1-x}Ge_x$ DBRTS due to index-nonconserving tunneling between Landau levels that cannot be attributed to scattering. We attribute these index-nonconserving peaks to strong Landau-level mixing and use the data to map out the energy spacing between Landau levels in strained $Si_{1-x}Ge_x$ quantum wells. A possible explanation for the surprising strength of the $\Delta n = 2$ level mixing is the large in-plane anisotropy of $Si_{1-x}Ge_x$, which we measured using $I(V, B_\perp)$ magnetotunneling as a function of $B_\perp$ orientation in the plane. We find the HH_0 subband to be highly anisotropic, with significantly smaller $E(k_\perp)$ curvature (heavier in-plane mass) in the $\langle 110 \rangle$ direction.

We are pleased to acknowledge the assistance of the Francis Bitter National Magnet Laboratory staff and D. Syphers. Work at IBM was partially supported by ONR (N0001492-C-0017).

1. References

[1] S. Luryi, Appl. Phys. Lett. 47 (1985) 490.
[2] E.E. Mendez, L. Esaki and W.I. Wang, Phys. Rev. B 33 (1986) 2893.
[3] V.J. Goldman, D.C. Tsui and J.E. Cunningham, Phys. Rev. B 35 (1987) 9387.
[4] V.J. Goldman, D.C. Tsui and J.E. Cunningham, Phys. Rev. B 36 (1987) 7635.
[5] L. Eaves, K.W.H. Stevens and F.W. Sheard, in: The Physics and Fabrication of Microstructures, Eds. M.J. Kelly and C. Weisbuch (Springer, New York, 1986) p. 343.
[6] R.A. Davies, D.J. Newson, T.G. Powell, M.J. Kelly and H.W. Myron, Semicond. Sci. Technol. 2 (1987) 61.
[7] A. Zaslavsky, Yuan P. Li, D.C. Tsui, M. Santos and M. Shayegan, Phys. Rev. B 42 (1990) 1374.
[8] E.E. Mendez, W.I. Wang, B. Ricco and L. Esaki, Appl. Phys. Lett. 47 (1985) 415.
[9] R.K. Hayden, L. Eaves, M. Henini, D.K. Maude, J.C. Portal and G. Hill, Appl. Phys. Lett. 60 (1992) 1474.
[10] H.C. Liu, D. Landheer, M. Buchanan and D.C. Houghton, Appl. Phys. Lett. 52 (1988) 1809.
[11] K.L. Wang, J. Park, S.S. Rhee, R.P. Karunasiri and C.H. Chern, Superlattices Microstruct. 5 (1989) 201.
[12] J.M. Luttinger, Phys. Rev. 102 (1956) 1030.
[13] G.E. Gurgenishvili, Fiz. Tverd. Tela 5 (1963) 2070 [Sov. Phys.–Solid State 5 (1964) 1510]; G.R. Khutsishvili, Fiz. Tverd. Tela 4 (1962) 2708 [Sov. Phys.–Solid State 4 (1963) 1986].
[14] D.A. Broido and L.J. Sham, Phys. Rev. B 31 (1985) 888; L.J. Sham, in: High Magnetic Fields in Semiconductor Physics, Ed. G. Landwehr (Springer, New York, 1987) p. 288.
[15] A. Zaslavsky, D.A. Grützmacher, Y.H. Lee, W. Ziegler and T.O. Sedgwick, Appl. Phys. Lett. 61 (1992) 2872 and references therein.
[16] E.P. O'Reilly and G.P. Witchlow, Phys. Rev. B 34 (1986) 6030.
[17] G. Schuberth, G. Abstreiter, E. Gornik, F. Schäffler and J.F. Luy, Phys. Rev. B 43 (1991) 2280.
[18] J.-P. Cheng, V.P. Kesan, D.A. Grützmacher and T.O. Sedgwick, Appl. Phys. Lett. 62 (1993) 1522.
[19] U. Gennser, V.P. Kesan, D.A. Syphers, T.P. Smith III, S.S. Iyer and E.S. Yang, Phys. Rev. Lett. 67 (1991) 3828.